Luciferin Derivatives for Enhanced in Vitro and in Vivo Bioluminescence Assays†

Rajesh Shinde,‡,§ Julie Perkins,§,|| and Christopher H. Contag*,‡,§

Department of Pediatrics, Radiology, and Microbiology and Immunology, Stanford University, Clark Center, 318 Campus Drive, Stanford, California 94305, Chemistry and Materials Science Directorate, Lawrence Livermore National Laboratory, 7000 East Avenue, Livermore, California 94551, and NSF Center for Biophotonics Science and Technology, University of California, Davis, 2700 Stockton Boulevard, Suite 1400, Sacramento, California 95817

Received March 9, 2006; Revised Manuscript Received June 2, 2006

ABSTRACT: In vivo bioluminescence imaging has become a cornerstone technology for preclinical molecular imaging. This imaging method is based on light-emitting enzymes, luciferases, which require specific substrates for light production. When linked to a specific biological process in an animal model of human biology or disease, the enzyme−substrate interactions become biological indicators that can be studied noninvasively in living animals. Signal intensity in these animal models depends on the availability of the substrate for the reaction within living cells in intact organs. The biodistribution and clearance rates of the substrates are therefore directly related to optimal imaging times and signal intensities and ultimately determine the sensitivity of detection and predictability of the model. Modifications of D-luciferin, the substrate for the luciferases obtained from beetle, including fireflies, result in novel properties and offer opportunities for improved bioassays. For this purpose, we have synthesized a conjugate, glycine−D-aminoluciferin, and investigated its properties relative to those of D-aminoluciferin and D-luciferin. The three substrates exhibited different kinetic properties and different intracellular accumulation profiles due to differences in their molecular structure, which in turn influenced their biodistribution in animals. Glycine−D-aminoluciferin had a longer in vivo circulation time than the other two substrates. The ability to assay luciferase in vitro and in vivo using these substrates, which exhibit different pharmacokinetic and pharmacodynamic properties, will provide flexibility and improve current imaging capabilities.

The luciferase enzyme (Luc)[1] from the North American firefly, *Photinus pyralis*, is widely used as a reporter in biochemical assays, in cell culture, and more recently in animal models (*1*). The versatility of this reporter system has been demonstrated through its use in studying gene expression, gene delivery, cell viability, cell physiology, in vivo cell trafficking, tumor burden, and protein−protein interaction (*1*). Luc catalyzes the conversion of the natural substrate D-luciferin, in the presence of oxygen, Mg^{2+}, and ATP, to oxyluciferin accompanied by release of a photon. The multistep reaction proceeds with the formation of a complex, Luc·D-luciferin-AMP, followed by the formation of excited oxyluciferin (Scheme 1) (*2*). The excited oxyluciferin then emits light with great efficiency upon relaxation (*3*, *4*). Bioluminescence imaging of cells and animals benefits greatly from extremely high signal-to-noise ratios relative to other imaging techniques, such as fluorescence, as cells and tissues do not emit significant light during normal cellular processes. Thus, improvements in the properties of the enzyme and the substrates will offer new opportunities for studying biology in vivo (*5*−*9*).

Numerous studies have measured Luc activity in cell lysates, live cells, and animals, but a thorough understanding of the optimal reaction conditions in all three settings and the properties of D-luciferin and its analogues that affect these conditions has not been reported. Ignowski et al. developed a model to determine Luc activity in living cells using human embryonic kidney cells (*10*). The model showed that the cell membrane does not present a major barrier for D-luciferin, and intracellular Luc decay is dependent on chaperones, which may vary between cell types. The Michaelis constant (K_m) for the bioluminescence reaction was found to be different for free and cellular Luc, which was attributed to factors such as intracellular enzyme inhibitors (pyrophosphate) or other entities sequestering the D-luciferin substrate. Lee et al. conducted extensive investigation of the biodistribution of D-luciferin in mice using radioiodine labeling techniques (*11*, *12*). The biodistribution of radiolabeled 7′-[^{123}I]iodo-D-luciferin was not identical to that of D-luciferin, and differing levels of the radiolabeled compound in various tissues were observed. This indicated that enhancement of biodistribution characteristics of the luciferase substrate would benefit imaging studies.

† This work was supported, in part, by funding from the National Science Foundation as part of the NSF Center for Biophotonics Science and Technology, a NSF Science and Technology Center at the University of California, Davis, under Cooperative Agreement PHY 0120999, and by the NIH (Grant R24 HD37543). This work was carried out under the auspicies of the U.S. Department of Energy by the University of California, Lawrence Livermore National Laboratory, under Contract W-7405-Eng-48.

* To whom correspondence should be addressed. E-mail: ccontag@stanford.edu. Telephone: (650) 725-8781. Fax: (650) 498-7723.

‡ Stanford University.

§ University of California, Davis.

|| Lawrence Livermore National Laboratory.

[1] Abbreviations: BLI, bioluminescence imaging; Luc, luciferase enzyme; PC3M, prostate cancer cells; CMV, cytomegalovirus.

10.1021/bi060475o CCC: $33.50
Published on Web 08/25/2006

Scheme 1: Mechanism of the Reaction between Luc and D-Luciferin

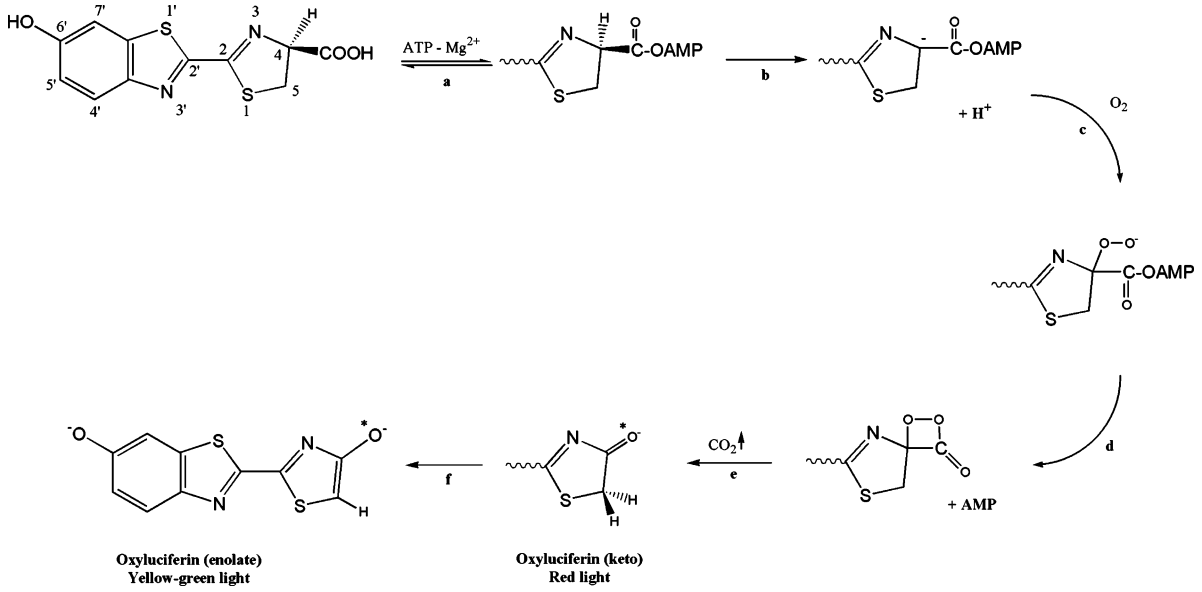

Effective bioluminescent imaging requires a good understanding of the pharmacokinetic and pharmacodynamic properties of the enzyme substrate in animal models. For example, the typical dose for mice is 150 mg/kg of body weight, and at this concentration, the substrate saturates the enzyme present in the cells provided that there are a limited number of cells expressing Luc in the model. This was indicated by demonstrating that increasing the dose did not increase the bioluminescence signal in mice carrying luciferase as a transgene where luciferase expression was activated in a small number of cells in the skin (*13*). However, this may not be true for studies of large tumors with compromised circulation or other situations where there is limited circulation or excessive reporter gene expression (*14*). The bioluminescent signal, depending on the tissue expressing Luc, typically peaks 15 min after injection and starts to decrease after 20 min (*13*), although for expression in the abdominal cavity or liver the signal may peak 5 min after injection of the substrate. Therefore, repeated substrate injections are required for temporal analyses, and suboptimal results are obtained if measurements are taken off the peak values. Attempts to stabilize the signals in bioluminescence imaging have been made using implantable osmotic pumps (*15*), but these approaches are inefficient and expensive.

For these reasons, Luc substrates that exhibit longer circulation times leading to more stable signals in vivo would further increase the number of types of studies that could be performed in vivo, reduce the costs of performing these studies, and eliminate some of the variability that can occur with repeated imaging over a 30−60 min time frame. This will be particularly important as three-dimensional imaging studies that require longer imaging times become routine (*16*). Here, we report the synthesis of a glycine−D-aminoluciferin conjugate. The kinetic and transport properties of this conjugate, D-luciferin, and D-aminoluciferin were investigated using firefly Luc as the reporter enzyme in four different environments: purified enzyme in buffer, cell lysates, live cells, and live animals. The different properties of the substrates that are being investigated will add greater flexibility to future in vitro and in vivo assay development.

EXPERIMENTAL PROCEDURES

General. Luciferin **1** (Figure 1) was purchased from Biosynth International. Aminoluciferin **2** (Figure 1) was obtained from Marker Gene Technologies (Eugene, OR). All other reagents were obtained from Sigma-Aldrich (St. Louis, MO), unless otherwise noted.

*Preparation of Glycine−D-Aminoluciferin Conjugate **3** (Figure 1) and Precursors.* 2-Chloro-6-nitrobenzathiazole was prepared using a method described by Katz (*17*). The compound was used in the subsequent step without purification. A small portion was purified by silica column chromatography (dichloromethane) for analysis. ^{1}H and ^{13}C NMR spectra were recorded on a Bruker DRX 500 MHz spectrometer. Splitting patterns are quoted as follows: s, singlet; d, doublet; m, multiplet. Mass spectra were acquired on a Micromass Quattro Micro API mass spectrometer operating in positive ion mode: ^{1}H NMR [$(CD_3)_2SO$, 500 MHz] δ 8.16 (d, J = 8.5 Hz, 1H), 8.38 (dd, J = 9.0, 2.5 Hz, 1H), 9.17 (dd, J = 2.5, 0.5 Hz, 1H); ^{13}C NMR [$(CD_3)_2SO$, 125 MHz] δ 119.5, 122.2, 123.0, 159.3, 136.5, 144.8, 154.2; ESI-MS of $C_7H_3ClN_2O_2S$ $[M + H]^+$ = 214.9, 216.9.

2-Chloro-6-aminobenzothiazole. 2-Chloro-6-aminobenzothiazole was prepared using a method described by Katz (*17*). The compound was used in the subsequent step without purification: ^{1}H NMR [$(CD_3)_2SO$, 500 MHz] δ 3.15 (br s, NH_2, 2H), 6.78 (d, J = 8.5 Hz, 1H), 6.97 (s, 1H), 7.68 (d,

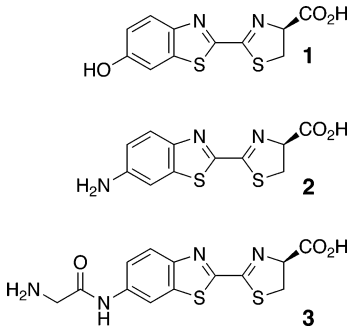

FIGURE 1: Luc substrates that were investigated: D-luciferin **1**, D-aminoluciferin **2**, and glycine−D-aminoluciferin **3**.

$J = 9.0$ Hz, 1H); ^{13}C NMR [$(CD_3)_2SO$, 125 MHz] δ 103.7, 115.0, 122.7, 137.4, 145.0, 147.7; ESI-MS of $C_7H_5ClN_2S$ $[M + H]^+ = 184.8, 186.8$.

2-Cyano-6-aminobenzothiazole. 2-Cyano-6-aminobenzothiazole was prepared and purified using a method described by White et al. (*18*). However, the purification of this molecule was not trivial. Repeated chromatography was required to purify the compound, which decreased the yield to 20−35%: ^{1}H NMR [$(CD_3)_2SO$, 500 MHz] δ 6.15 (br s, NH_2, 2H), 6.98 (dd, $J = 9.0$, 2.5 Hz, 1H), 7.17 (d, $J = 2.5$ Hz, 1H), 7. 88 (d, $J = 9.0$ Hz, 1H); ^{13}C NMR [$(CD_3)_2SO$, 125 MHz] δ 102.2, 114.3, 117.3, 125.1, 127.5, 138.3, 143.2, 150.4; ESI-MS of $C_8H_5N_3S$ $[M + H]^+ = 175.9$.

2-Cyano-6-amino-N-Boc-glycine-benzothiazole. To produce 2-cyano-6-amino-*N*-Boc-glycine-benzothiazole, 60 mg (0.34 mmol) of Boc-glycine was dissolved in 2 mL of dry THF; 75 μL (0.68 mmol) of *N*-methylmorphiline, followed by 57 μL (0.44 mmol) of isobutyl chloroformate, was added portionwise at 0 °C. The reaction mixture was stirred at 0 °C in the dark for 30 min after which 60 mg (0.34 mmol) of 2-cyano-6-aminobenzothiazole dissolved in 1 mL of dry THF was added portionwise over the course of 30 min. The reaction mixture was kept at 0 °C for a further 2 h, followed by 16 h at room temperature in the dark. Analytical HPLC and mass spectrometry analysis (ESI-MS of $C_{15}H_{16}N_4O_3S$ $[M + H]^+ = 332.9$) showed complete conversion to the product. Analytical HPLC of the Boc-protected intermediate showed a peak at 4.4 min [10 min linear gradient from 50% water (0.1% TFA) to 80% acetonitrile (0.1% TFA)]. Saturated $KHCO_3$ was added to quench any remaining isobutyl chloroformate, and the reaction mixture was evaporated to dryness. The residue was redissolved in ethyl acetate, and the organic phase was washed twice with saturated $KHCO_3$ and once with saline solution and dried with $MgSO_4$. The ethyl acetate was evaporated and the product isolated by normal phase flash chromatography (100% dichloromethane to 98% dichloromethane and 2% methanol). The yellow solid was analyzed by NMR spectroscopy and contained a small number (<5%) of impurities but was used in the next step without further purification because more stringent HPLC purification could remove the Boc group and reduce the yield and efficiency of subsequent steps: ^{1}H NMR (CD_3OD, 500 MHz) δ 8.58 (s, 1H), 8.05 (d, $J = 9.0$ Hz, 1H), 6.98 (d, $J = 9.0$ Hz, 1H), 5.48 (s, 1H), 3.92 (br s, 2H), 1.48 (s, 9H); ^{13}C NMR (CD_3OD, 125 MHz) δ 27.8, 44.3, 111.7, 113.1, 121.1, 124.9, 125.6, 148.8, 169.9; ESI-MS of $C_{15}H_{16}N_4O_3S$ $[M + H]^+ = 332.9$, tBu of Boc group $[M + H]^+ = 276.9$.

Glycine−D-Aminoluciferin. 2-Cyano-6-amino-*N*-Boc-glycine-benzothiazole (112 mg, 0.34 mmol) was dissolved in 2 mL of DMF; 71 mg (0.41 mmol) of H-D-cysteine·HCl was dissolved in 300 μL of degassed water and the mixture adjusted to pH 8.0 by addition of saturated K_2CO_3 in degassed water (*19*). The D-cysteine solution was added dropwise in the dark to the organic solution, and the reaction mixture was stirred for 1 h at room temperature in the dark. Analytical HPLC and mass spectrometry analysis (ESI-MS of $C_{18}H_{20}N_4O_5S_2$ $[M + H]^+ = 437.0$) showed complete conversion to the product. Analytical HPLC of the Boc-protected product showed a single peak at 8.5 min [10 min linear gradient from 50% water (0.1% TFA) to 80% acetonitrile (0.1% TFA)]. The reaction mixture was evaporated to dryness. The residue was redissolved in a mixture of ethyl acetate and a small amount of methanol (to help solubility) and any solid residue removed by filtration through a 0.22 μm filter. The organic solvent was removed be evaporation and dried under high vacuum. The Boc group was removed by treatment with dichloromethane, 20% TFA, and 1% Et_3SiH for 1 h. The solvent was removed under vacuum, and analytical HPLC showed a single peak at 5.4 min [10 min linear gradient from 95% water (0.1% TFA) to 80% acetonitrile (0.1% TFA)]. The crude product was isolated by semipreparative HPLC [25 min gradient from 90% water (0.1% TFA) to 40% acetonitrile (0.1% TFA)] and lyophilized to dryness to give 75 mg of final product as a pale yellow solid (65% over two steps). A small amount of inseparable impurity was evident in the analytical HPLC results of the final product (Figure 1 of the Supporting Information), and the purity is estimated to be 95%: ^{1}H NMR [$(CD_3)_2SO$, 500 MHz] δ 3.67−3.83 (dd, $J = 36.0$, 9.0 Hz, 2H), 3.86 (br s, 2H), 5.44 (dd $J = 9.0$ Hz, 1H), 7.66 (dd, $J = 9.0$, 2.0 Hz, 1H), 8.15 (d, $J = 9.0$ Hz, 1H), 8.20 (br s, 2H), 8.56 (d, $J = 2$ Hz, 1H), 10.85 (s, 1H); ^{13}C NMR [$(CD_3)_2SO$, 125 MHz] δ 34.7, 41.1, 78.1, 111.7, 119.5, 124.5, 136.4, 137.4, 148.9, 159.6, 164.4, 165.2, 171.0; ESI-MS of $C_{13}H_{12}N_4O_3S_2$ $[M + H]^+ = 336.8$.

Spectroscopic Characterization of Substrates. The absorption spectra for the three substrates were acquired using a SpectraMax-Plus microplate spectrophotometer (Molecular Devices) (Figure 2 of the Supporting Information). The fluorescence and bioluminescence spectra were aquired using a Spectra MAX Gemini EM fluorescence/luminescence plate reader (Molecular Devices) (Figures 3 and 4 of the Supporting Information, respectively). The measurements were taken in 40 mM Tris-acetate buffer [1 mM EDTA and 0.2 M NaCl (pH 7.7)]. The bioluminescence spectra were obtained using pure Luc enzyme (Promega Corp., Madison, WI). All spectra were recorded at room temperature.

Imaging. Photon emission was measured using an IVIS 200 device (Xenogen Corp., Alameda, CA). The IVIS 200 device consists of a cooled integrating CCD camera mounted on a dark specimen chamber, a camera controller, and a camera cooling system. Bioluminescence measurements of luciferase activity were acquired at short intervals as described in the figure legends. Different substrates required different exposure times with the displayed data adjusted for each substrate as indicated by the scale bar in each image. The temperature of the stage inside the imaging chamber was maintained at 37 °C. Light outputs from regions of interest (ROI) were quantified using LivingImage version 2.5 (Xenogen Corp.) as an overlay on Igor imaging analysis software (WaveMetrics, Lake Oswego, OR). The final light output, in photons per second, is a value that is normalized to the integration time, the distance from the camera to the animal and/or plate, the instrument gain, and the solid angle of measurement (*20*, *21*). The data are represented as pseudocolor images of light intensity where red is the most intense and blue is the least intense.

Luciferase Enzyme Assays. Purified Luc was obtained from Promega Corp. The substrates were prepared in bioluminescence buffer [40 mM Tris-acetate, 1 mM EDTA, 1 mM DTT, 3.45 mM ATP, 0.2 M NaCl, 5.7 mM $MgSO_4$, and 0.76 mM coenzyme A (pH 7.6)]; 100 μL of the substrate was added to 10 μL of a Luc enzyme solution (1 ng/μL). All the assays

were carried out in triplicate, and the photoemission was measured over 15 min using the IVIS 200 device.

Cell Lysate Assays. PC3M-Luc cells were lysed using passive lysis buffer (Promega Corp.), centrifuged to remove the cell debris, and stored in aliquots at −80 °C; 10 μL of the cell lysate solution was equivalent to 3×10^4 lysed PC3M-Luc cells. Substrates **1**−**3** were prepared in bioluminescence buffer; 100 μL of the substrate solution was added to 10 μL of freshly thawed cell lysate, and photon emission was measured using the IVIS 200 device. All the assays were carried out in triplicate.

Cell Culture. Human prostate cancer cells, PC3M previously engineered to constitutively express Luc from the immediate early promoter from cytomegalovirus (PC3M-Luc) (*22*), were maintained at 37 °C in 5% CO_2 in RPMI containing 10% FBS (Invitrogen, Carlsbad, CA), 100 units/mL penicillin, and 0.1 mg/mL streptomycin. These cells were used to investigate the influence of cellular membranes on substrate transport.

Live Cell Assays. Live PC3M-Luc cells were assayed in black 96-well plates. The plates were seeded with known amounts of PC3M-Luc cells and placed overnight in an incubator. Subsequently, medium was replaced with HBSS buffer without phenol red (Invitrogen) containing 2% FBS and 0.1 mg/mL cycloheximide and incubated at 37 °C for 100 min. The three substrates were prepared at different concentrations in HBSS (0.1 mg/mL cycloheximide and 2% FBS). The wells were cleared of the medium just before measurements and replaced with 100 μL of the substrate solution; cyclohexamide prevents new protein synthesis and controls fluctuations in the expression of luciferase. Photoemission was measured using the IVIS 200 device. Experiments were carried out in triplicate. The substrate concentration was varied from 3 to 500 μM for all substrates.

Animal Imaging. Transgenic reporter FVB/L2G85 mice (*23*) constitutively express the luciferase gene from the minimal β-actin promoter with a CMV enhancer such that all cells and tissues express detectable levels of luciferase. These mice were anesthetized using isofluorene and were given 200 μL of substrates at a concentration of 1 mM via injection into the intraperitoneal cavity. This concentration is significantly lower than the concentration of D-luciferin (107 mM) that is typically used in small animal imaging studies. Photon emission from the ROI (entire animal) was measured using the IVIS 200 device.

RESULTS AND DISCUSSION

The spectral properties of the three substrates shown in Figure 1, natural Luc substrate D-luciferin **1** and two derivatives (D-aminoluciferin **2** and glycine−D-aminoluciferin **3**), were investigated. The bioluminescence reaction was also investigated under four different conditions: purified Luc in buffer, cell lysates, live cells, and live animals. Purified Luc provided information about Luc·substrate kinetics. Cell lysates yielded information about the influence of intracellular enzymes on Luc·substrate kinetics, whereas live cell assays provided insight into the influence of the cell membrane and intracellular enzyme compartmentalization on the kinetics of the reaction. Substrate biodistribution in mice was used to determine the effects of substrate biodistribution, clearance rates, and membrane transport on Luc·substrate kinetics. A mechanism for the bioluminescence reaction for firefly luciferase and D-luciferin proposed previously (*2*, *24*) is shown in Scheme 1 with D-luciferin as the substrate. Luc catalyzes the formation of enzyme-bound D-luciferin adenylate. This is followed by deprotonation of the adenylate and subsequent addition of an oxygen molecule to the resultant anion. Cyclization and elimination of CO_2 result in the formation of an electronically excited-state oxyluciferin intermediate (oxyluciferin*). Relaxation of the excited state of oxyluciferin to the ground state is accompanied by the emission of photons. The light emission via this process, using D-luciferin as a substrate, has a quantum yield of ∼0.9 (*3*) and demonstrates the highly efficient catalysis and radiative decay of oxyluciferin* by Luc.

Spectroscopic Characterization of Substrates. The three substrates were characterized for absorbance, fluorescence, and bioluminescence. D-Luciferin, D-aminoluciferin, and glycine−D-aminoluciferin exhibited absorbance peaks at 330, 350, and 327 nm, respectively. The measurements were normalized to 1 and accounted for background from the buffer (Figure 2 of the Supporting Information). The fluorescence measurements for the three substrates were acquired by excitation at 324 nm (D-luciferin and glycine−D-aminoluciferin) and 350 nm (D-aminoluciferin). Emission peaks were observed at 530 nm (D-luciferin), 520 nm (D-aminoluciferin), and 450 nm (glycine−D-aminoluciferin), as shown in Figure 3 of the Supporting Information. The lower-fluorescence emission peak for glycine−D-aminoluciferin could be due to the lower ionization level of the glycine group. Similar results were reported for 6-methoxy analogues of D-luciferin (*24*). The bioluminescence spectra exhibited peaks at 560 nm (D-luciferin), 578 nm (D-aminoluciferin), and 570 nm (glycine−D-aminoluciferin) as shown in Figure 4 of the Supporting Information. Zhao et al. reported the emission spectra of Luc·D-luciferin bioluminescence in live cells and animals and observed a shift in the emission peak when the reaction temperature was increased from 25 to 37 °C (*25*). Similar shifts in the emission wavelengths were previously reported for D-luciferin at higher temperatures or lower pH (*24*, *26*).

Luciferase Enzyme Assays. The IVIS 200 device outputs the rate of photon emission by bioluminescence reactions in photons per second. Photon emission is proportional to the amount of product (e.g., oxyluciferin* for D-luciferin) formed in a bioluminescent reaction. The photon emission rate was multiplied by the time period between measurements, to give the total photons emitted in each period. Addition of these photons collected in each time period yielded a cumulative profile of the bioluminescence product formed over the course of a bioluminescent reaction. Figure 2a shows a representative example of the cumulative photons emitted over time for D-luciferin with Luc. The slope of these curves under steady-state conditions gave the rate of product formation, v, at different initial substrate concentrations. Figure 2b shows the rate of product formed, v, with an increasing substrate concentration, S.

The total photons emitted is proportional to the amount of product formed (e.g., release of light from oxyluciferin* when D-luciferin is the substrate). Michaelis−Menten enzyme kinetics calculations (eq 1) were applied to the results in Figure 2b to determine the Michaelis−Menten constant (K_m)

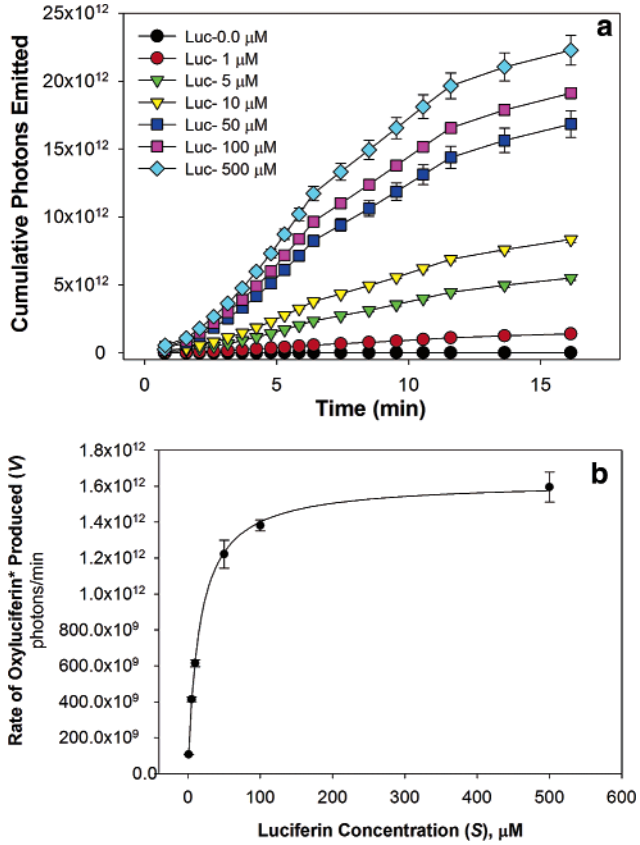

FIGURE 2: Luc·D-luciferin kinetics of purified Luc at different initial substrate concentrations (from 0.0 to 500 μM). Ten microliters of the solution contains 10 ng of Luc. (a) Cumulative number of photons emitted by the reaction at various times. The slopes of the curves provide the rate of product formation, v, in photons per second at different substrate concentrations, and the result is shown in panel b. The data are fit to the Michaelis−Menten equation (eq 1).

Table 1: Kinetic Parameters for the Purified Luciferase Enzyme

substrate	K_m (μM)	V_{max} ($\times 10^9$ photons/min)	V_{max}/K_m ($\times 10^9$ photons min^{-1} μM^{-1})
D-luciferin **1**	16 ± 1.0	1626 + 24	102
D-aminoluciferin **2**	0.62 + 0.05	169 ± 2.6	272
glycine−D-aminoluciferin **3**	114 + 12	9.2 ± 0.5	0.08

and the maximum rate of product formation, V_{max} (photons per minute), for all three substrates (Table 1).

$$v = \frac{V_{max}S}{K_m + S} \quad (1)$$

The K_m values indicate that D-aminoluciferin has the highest affinity for Luc followed by D-luciferin and glycine−D-aminoluciferin, whereas the V_{max} values show that D-luciferin achieves the highest rate of photon emission, followed by D-aminoluciferin and glycine−D-aminoluciferin. Taken together (Table 1, V_{max}/K_m which is proportional to K_{cat}/K_m), Luc exhibits a higher catalytic efficiency for D-aminoluciferin followed by D-luciferin. Glycine−D-aminoluciferin exhibits a lower affinity for Luc apart from a lower V_{max}. Since light is produced only by the excited-state intermediate, the lower V_{max} values of D-aminoluciferin and glycine−D-aminoluciferin may indicate catalytic turnover slower than and radiative efficiencies lower than those of

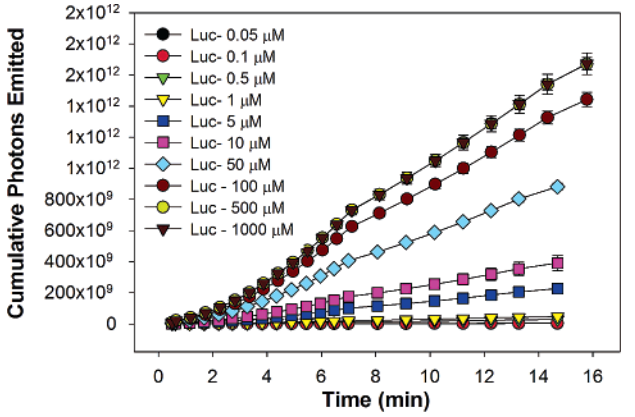

FIGURE 3: Luc·D-luciferin kinetics of PC3M-Luc cell lysates at different initial substrate concentrations (from 0.05 to 1000 μM). Ten microliters of the lysate corresponds to 30 000 cells. Cumulative number of photons emitted by the reaction at various times.

Table 2: Kinetic Parameters for PC3M-Luc Cell Lysates

substrate	K_m (μM)	V_{max} ($\times 10^9$ photons/min)	V_{max}/K_m ($\times 10^8$ photons min^{-1} μM^{-1})
D-luciferin **1**	34 ± 3.0	120 ± 2.0	36
D-aminoluciferin **2**	0.9 ± 0.1	23 ± 0.6	268
glycine−D-aminoluciferin **3**	8.7 ± 3.2	6.5 ± 0.1	7.5

D-luciferin. The formation of the excited-state intermediate is also dependent on the rate of substrate adenylation and adenylate oxidation (Scheme 1). Hence, the differences in the kinetic parameters observed between the three substrates could be a result of any or all of these steps.

Whereas the carboxylic acid on the thiazole ring, where the reaction takes place to form oxyluciferin, is the same for all three substrates, the three substrates have different electronic properties, and this may affect their interaction with amino acid residues in the enzyme pocket. The phenolic group in the 6-position of D-luciferin is an anion at physiological pH. Therefore, in solution at a relevant pH, D-luciferin has a net overall charge of −2. D-Aminoluciferin, with an aniline nitrogen in the 6-position, has an overall charge of −1 under similar conditions. Since the pK_a of the glycine amine group is 9.8 and an aniline nitrogen has a pK_a of ∼4.6, glycine−D-aminoluciferin, an amino acid conjugate, is likely to exist as a zwitterion at physiologic pH. In addition, all three substrates have very different hydrogen bonding capabilities. Glycine−D-aminoluciferin is substantially larger, and therefore, a steric effect may also influence the overall enzyme−substrate binding affinity. The combination of different noncovalent and steric interactions for all three substrates is likely to contribute to the differences in the observed kinetic parameters.

Cell Lysates. The photon emission measurements for cell lysates were converted to cumulative photon emission at different times for the three substrates (Figure 3), as described in the previous section, and the rate of production of the excited-state substrate at different substrate concentrations was obtained. Application of the Michaelis−Menten equation (eq 1) provided the kinetic parameters (Table 2). The calculated K_m values were in the following order: D-luciferin > glycine−D-aminoluciferin > D-aminoluciferin. Glycine−D-aminoluciferin exhibited a decrease in the measured K_m in cell lysate, whereas the K_m for D-luciferin increased to 34

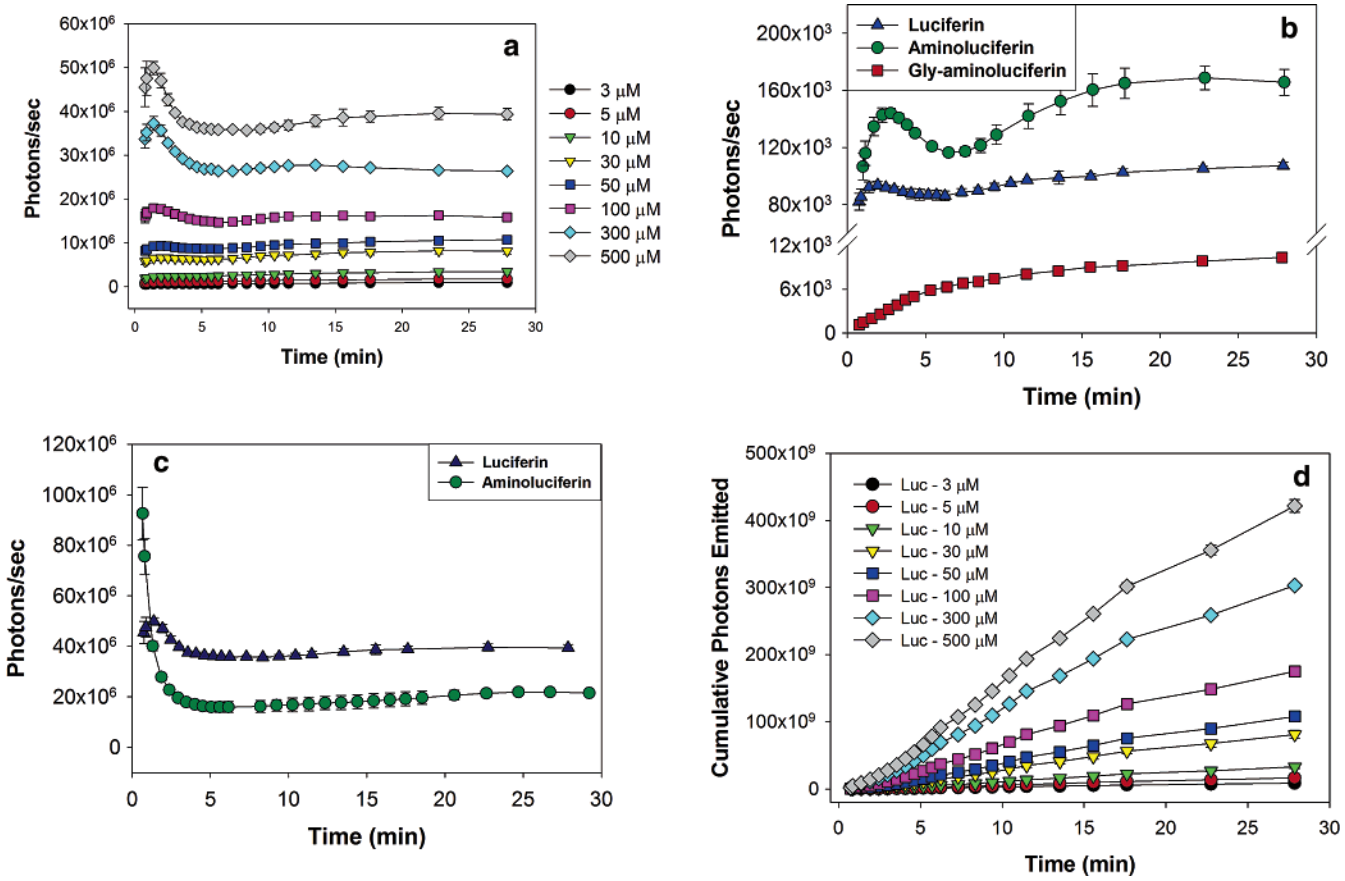

FIGURE 4: Luc•D-luciferin kinetics in PC3M-Luc live cells. Transport of D-luciferin across 30 000 PC3M-Luc cells at different initial D-luciferin concentrations (from 3 to 500 μM), as observed from the emission of photons. Cells were preincubated for 100 min in 0.1 mg/mL cycloheximide in medium (HBSS with 2% FBS). The volume of substrate was 100 μL. (a) Photons collected with the IVIS 200 device from the cells at different times. The curves show an initial peak at ~2 min before reaching a plateau. (b and c) Comparison of photon emission profiles from PC3M-Luc cells for the substrates at two different concentrations: (b) 50 μM D-luciferin, D-aminoluciferin, and glycine−D-aminoluciferin and (c) 500 μM D-luciferin and D-aminoluciferin. (d) Cumulative number of photons emitted by the cells at various times.

μM, compared to value obtained from purified Luc in buffer. D-Aminoluciferin did not exhibit an appreciable change in its K_m value for the PC3M-Luc cell lysates. The decrease in the K_m for glycine−D-aminoluciferin could be attributed to the presence of intracellular enzymes in the cell lysate. Glycine is attached to the amine group of D-aminoluciferin via an amide bond. This amide bond could be a potential target for some intracellular enzymes and release free D-aminoluciferin and glycine. This hypothesis was further supported after considering the relative V_{max} of the three substrates under the different conditions. Whereas D-luciferin still exhibited the highest V_{max}, the difference in value with D-aminoluciferin decreased 2-fold in the cell lysate. The difference in the V_{max} values between D-luciferin and glycine−D-aminoluciferin decreased 10-fold in the cell lysate. D-Aminoluciferin has a low K_m; hence, even small amounts of free D-aminoluciferin generated from the intracellular enzymatic breakdown of glycine−D-aminoluciferin can impact the observed K_m for glycine−D-aminoluciferin while simultaneously increasing V_{max}. The V_{max}/K_m ratios show that the Luc enzyme present in the cell lysates catalyzes D-aminoluciferin more efficiently than D-luciferin and glycine−D-aminoluciferin, and this is similar to observations made with purified Luc in buffer. The relative difference in V_{max}/K_m values between D-aminoluciferin and D-luciferin appeared to increase, due to an increase in K_m for D-luciferin. An increase in observed K_m values for D-luciferin has been attributed by Ignowski et al. to pyrophosphates in the cell lysates, which have been shown by Gandelman et al. to affect the activity of Luc (*10*, *27*). Denburg et al. (*28*) showed that ATP, AMP, pyrophosphate, and phosphate influence D-luciferin binding characteristics. The relative difference in V_{max}/K_m values between D-aminoluciferin and glycine−D-aminoluciferin decreased significantly. The increase in V_{max}/K_m for glycine−D-aminoluciferin could be attributed to the presence of free D-aminoluciferin released by the enzymatic action of the intracellular proteins.

Live Cells. PC3M-Luc cells express Luc constitutively (*22*). To compare kinetic data from PC3M-Luc live cells and cell lysate, the intracellular Luc concentration was kept constant. This was achieved by exposing PC3M-Luc cells to cycloheximide, which inhibits protein synthesis but does not interfere with Luc activity (*10*, *29*). After incubation with cycloheximide, the medium was replaced with substrate solutions (with cycloheximide) and the photon emission was measured. The substrates may localize to different subcellular compartments upon transport across the membrane. The photons emitted from the cells represent the interaction with Luc which is present predominantly in the cytoplasm. Figure 4a shows a representative example of the rate of photons emitted at increasing concentrations of D-luciferin, measured over 28 min (to ensure that steady-state photon emission was

Table 3: Kinetic Parameters for PC3M-Luc Cells

substrate	K_{m-eff} (μM)	$V_{max-eff}$ ($\times 10^7$ photons/min)	$V_{max-eff}/K_{M-eff}$ ($\times 10^6$ photons min^{-1} μM^{-1})	S_{c-max} (μM)
D-luciferin **1**	235 ± 20	2669 ± 39	113.6	7.4 ± 0.3
D-aminoluciferin **2**	141 ± 23	294 ± 43	20.5	0.1 ± 0.01
glycine−D-aminoluciferin **3**	62 ± 6	7.4 ± 0.6	1.2	0.1 ± 0.005

attained). The rate of photons emitted shows an initial peak at ~2 min before it drops to a steady value. This peak is most likely due to an initial burst of enzymatic activity represented by the formation of the Luc·oxyluciferin* complex, which is proportional to the substrate present intracellularly. Subsequently, the trough and stable region of the curve may reflect the kinetic phase during which the complex decomposes back to free Luc and product. The substrate is transferred in and out of the cell, and its concentration equilibrates across the cell membrane as a function of concentration and/or membrane potential. During the initial burst in Luc·oxyluciferin* formation, there could also be a rapid depletion of the intracellular substrate, causing a subsequent drop in the number of photons emitted. Subsequently, the system achieves a balance between the diffusion of the substrate, formation of the Luc·oxyluciferin* complex, and release of the product. These results imply that in live cells, the diffusion of luciferin across the membrane is the rate-limiting step. Similar behavior was observed in the case of D-aminoluciferin, but glycine−D-aminoluciferin exhibited a different photon emission profile. Figure 4b shows the rate of photon emission from all three substrates at an exogenous substrate concentration of 50 μM. D-Aminoluciferin achieves a higher Luc activity at lower concentrations due to a lower K_m which may explain the higher-magnitude bioluminescence signal compared to those of D-luciferin and glycine−D-aminoluciferin. At higher concentrations, when greater amounts of the substrate accumulate inside the cell, the light output from D-luciferin is higher than that of D-aminoluciferin, as shown in Figure 4c. The higher initial value for D-aminoluciferin observed in the figure confirms that the initial phase of the process (peak) is influenced by the formation of the Luc·oxyaminoluciferin* complex, as D-aminoluciferin binds to Luc more rapidly than D-luciferin. Subsequently, the emission from D-aminoluciferin drops to levels lower than those of D-luciferin, which indicates that at equilibrium, the intracellular concentration of D-aminoluciferin is significantly lower than that of D-luciferin. At glycine−D-aminoluciferin concentrations greater than 100 μM in the cell media, the substrate had a tendency to precipitate, and therefore, results for a higher concentration were not considered. From the luciferase enzyme experiments, it was observed that the formation of oxyglycine−D-aminoluciferin* from glycine−D-aminoluciferin is a very slow process. If this is a rate-limiting step, then glycine−D-aminoluciferin will not be exhausted rapidly within the cell during the initial few minutes, and hence, an initial peak with a subsequent dip will not be observed. In our experiments, no initial peak was observed for glycine−D-aminoluciferin.

As demonstrated by Gentry and co-workers (*30*), a macroscopic model for simple diffusion-controlled substrate delivery can be represented by replacing K_m and V_{max} in eq 1 with "effective" kinetic parameters, K_{m-eff} and $V_{max-eff}$, respectively. The catalytic efficiency, $V_{max-eff}/K_{m-eff}$, was shown to be the product of the efficiency of the enzyme when complexed with its substrate, ease of enzyme binding, and an additional parameter, the substrate diffusion rate (*30*). To study the influence of diffusion and/or facilitated transport of the three substrates across the cell membrane on the intracellular reaction kinetics, we applied eq 1 to the cell data, which is similar to the treatment of Luc and PC3M cell lysates. The K_{m-eff} and $V_{max-eff}$ values for the intracellular reaction with each substrate were calculated and are listed in Table 3. In this experimental setup, it was not possible to directly measure the intracellular concentration of the substrates, but a qualitative picture of the reaction kinetics inside live cells was determined from the kinetic parameters that were obtained. The rate of product formed in 30 000 PC3M-Luc cells (v) was determined from the cumulative photons emitted at different substrate concentrations in the cell culture medium. To estimate the substrate concentration inside the cells, certain assumptions were made. It is reasonable to assume that there is a loss of photons detected due to scattering and absorption from the cell membrane or other constituents in the cell. However, since the cells were a monolayer, this loss was not a significant portion of the total photons emitted by the cells and was constant for all experiments, assuming the number of cells in each well was the same. The cumulative number of photons emitted by cell lysate after 15 min (Figure 2a) was 10−50 times greater than the number emitted by the live PC3M-Luc cells (Figure 3d). Since the number of photons emitted is proportional to the substrate concentration, the intracellular substrate concentration appears to be much lower than the exogenous substrate concentration. Assuming that the V_{max} and K_m parameters calculated from the cell lysate experiments hold true for the bioluminescence reaction in live cells, the intracellular concentration for each substrate (S_c) was calculated from the Michaelis−Menten equation (eq 1). To obtain the maximal level of intracellular accumulation of substrate (S_{c-max}), the $V_{max-eff}$ was used for v in eq 1. Table 3 lists the calculated S_{c-max} values; D-luciferin exhibited the highest intracellular substrate concentration of the three substrates. It should be noted that all calculations for glycine−D-aminoluciferin are influenced by the intracellular enzymes that release D-aminoluciferin and hence do not represent an exact value. The results indicate that D-luciferin exhibits better intracellular accumulation.

The difference between the values calculated from the cell lysates and live cell experiments give an estimate of the effect of the cell membrane as a barrier to substrate and possible sequestration of the enzyme in cellular compartments. The rate of diffusion could have a significant impact on the K_{m-eff} values of the substrates. As observed in Table 3, D-aminoluciferin had a substantially higher K_{m-eff} value (166-fold) relative to its K_m in cell lysates, whereas the increase in K_{m-eff} for glycine−D-aminoluciferin and D-luciferin was ~7-fold in whole cells. Glycine−D-aminoluciferin has a lower observed K_m in cell lysates as a result of intracellular

cleavage and release of D-aminoluciferin (discussed in the previous section). If glycine−D-aminoluciferin encounters the same intracellular enzymes inside the cytoplasm of the cells, the relative increase in its K_{m-eff} (compared to that in cell lysate) may be due to slower transport across the cellular membrane. The catalytic efficiency (V_{max}/K_{m-eff}) (*30*) has been shown to be proportional to the rate of diffusion. Table 3 shows that the V_{max}/K_{m-eff} of D-luciferin is 7.4 times higher than that of D-aminoluciferin and 95 times higher than that of glycine−D-aminoluciferin. Comparion of the V_{max}/K_{m-eff} values of the three substrates in live cells (Table 3) and in cell lysates (Table 2) supports the argument that the movement of the three substrates is limited by the cell membrane. The catalytic efficiency is reduced 32-, 1300-, and 625-fold for D-luciferin, D-aminoluciferin, and glycine−D-aminoluciferin, respectively, in live PC3M cells. Intrinsic to these values is the influence of the cell membrane on the transport of the substrates, with D-luciferin exhibiting the highest level of intracellular accumulation followed by glycine−D-aminoluciferin and D-aminoluciferin. The catalytic efficiency for the live cells, $V_{max-eff}/K_{m-eff}$, showed that D-luciferin replaced D-aminoluciferin as a more efficient substrate at higher concentrations. As reported above, at lower concentrations, D-aminoluciferin was the brighter substrate. Interpretation of the $V_{max-eff}/K_{m-eff}$ for glycine−D-aminoluciferin is complicated by intracellular enzymes, but when compared to cell lysate data, these data suggest that the cell membrane is a significant barrier for transport. It should be noted that the release of D-aminoluciferin from the glycine−D-aminoluciferin conjugate is advantageous as this provides a mechanism for the slow release of D-aminoluciferin, thus prolonging the bioluminescence signal. The mechanism of glycine−D-aminoluciferin transport is under further investigation.

Live Animals. A representative image of a transgenic reporter mouse to which D-luciferin had been administered is shown in Figure 5a. The quantitative results from the animal biodistribution studies are shown in Figure 5b. The rates of total photons emitted from the whole animal are plotted as a function of time. After intraperitoneal injection, the substrate undergoes numerous intercellular transfers as it spreads across the body and is affected by Luc present in cells throughout the animal. Since the animals were transgenic and the luciferase was expressed by a ubiquitous constitutive promoter (all cells examined), the substrates could also encounter Luc while being transported by the blood cells, leading to signals from these cells. Each intercellular transport introduces a time delay that is a function of the transport properties of the substrates. Depending upon the imaging application, it may be necessary to have a fast-distributing or long-circulating substrate. Typically for temporal analysis, a substrate that emits the strongest signal for the longest time is preferred. Since the animals were transgenic for a highly expressed luciferase gene, they produced substantial quantities of the enzyme, and it was virtually impossible to supply enough substrate to reach saturation levels. It could be argued that the concentration of substrates injected in these experiments was significantly lower than the K_m value of each of the substrates by the time it reaches the cells. Since the substrate concentration interacting with Luc is low, mice to which D-aminoluciferin had been administered should emit a higher-

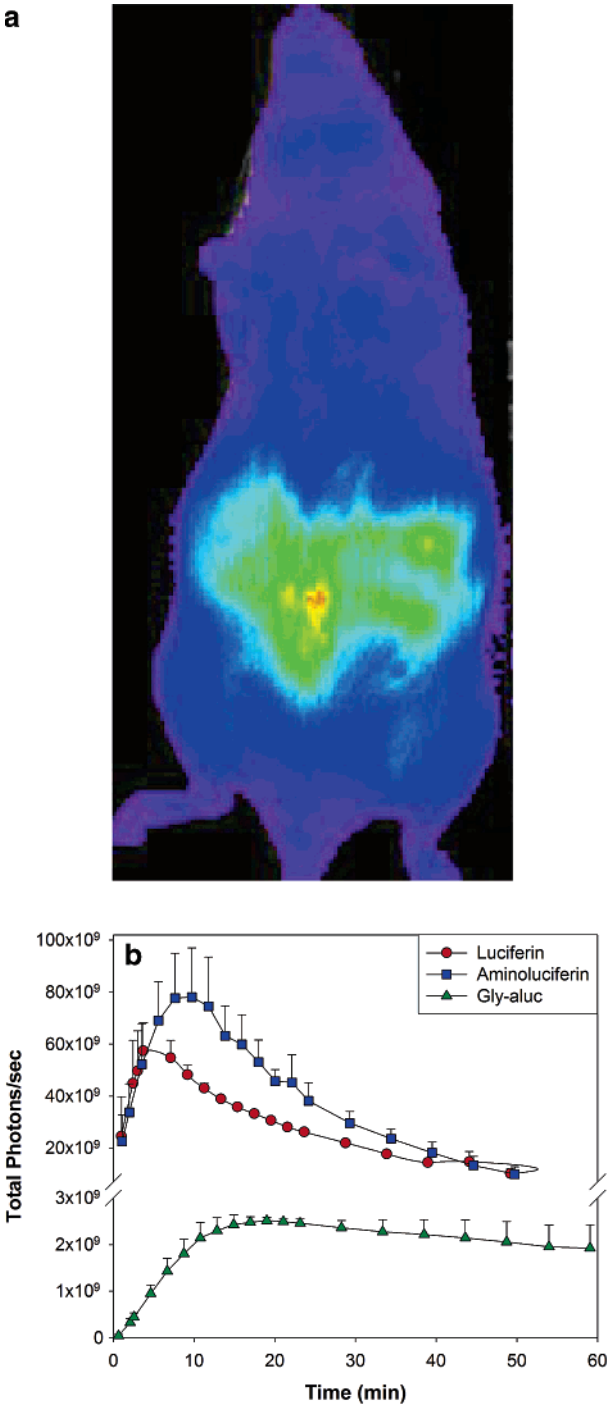

FIGURE 5: Three substrates were administered to mice. The mice (L2G85) were an FVB strain modified to constitutively express Luc uniformly with a β-actin promoter. Each mouse was injected intraperitoneally with 200 μL of the substrates at a concentration of 1 mM. (a) Bioluminescence images of L2G85 mice acquired with an IVIS 200 device for the three substrates. The images shown are for the maximum photon emission attained at the injected substrate concentrations. (b) Total number of photons emitted from the mice with the three substrates ($n = 3$).

magnitude signal (similar to PC3M-Luc data in Figure 4b). This is potentially why the D-aminoluciferin peak photon emission rate was ~25% higher than that of D-luciferin. The D-aminoluciferin curve is also broader due to a slower transport across cell membranes in comparison to that of D-luciferin. In comparison, glycine−D-aminoluciferin exhibited a much longer lasting signal with a peak emission

that was 20−30 times lower than those of the other two substrates. The longer duration of the glycine−D-aminoluciferin is a result of the slow transport across the cell membrane and a lower V_{max}/K_m. Once glycine−D-aminoluciferin reaches the interior of the cell, intracellular enzymes act upon it to release D-aminoluciferin. Thus, the photons emitted are a result of glycine−D-aminoluciferin and D-aminoluciferin. A longer-emitting substrate such as glycine−D-aminoluciferin is useful in certain applications, such as three-dimensional bioluminescence animal imaging and when the substrate needs to be delivered intravenously. When delivered intravenously, glycine−D-aminoluciferin was observed to peak at 10 min compared to a peak at ∼2 min for D-luciferin and D-aminoluciferin, which is useful in reducing measurement errors. Three-dimensional bioluminescence animal imaging is an emerging technology that involves generation of a tomographic three-dimensional reconstuction of the bioluminescent signal from an animal. The currently used substrate, D-luciferin, reaches a peak photon emission 15−20 min after injection, whereas each tomography scan can require imaging times of ≥10 min. Hence, a longer-circulating substrate such as glycine−D-aminoluciferin could be useful, especially for approaches that require long integration times or studies of temporal changes in signal over a 30−90 min time period.

CONCLUSIONS

Three substrates have been investigated using the purified Luc enzyme, in cell lysates, live cells, and animals. Manipulation of the substrate structure can be used to tailor the pharmacokinetic and pharmacodynamic properties. The enzymatic cleavage of glycine−D-aminoluciferin by intracellular enzymes to release D-aminoluciferin can be particularly useful in adapting the properties of the substrate to specific applications. The synthesis and use of glycine−D-aminoluciferin will be used as a model for future studies of enhanced bioluminescent substrates. This can be used to pursue appropriate biological questions in live cells or living animals. With careful design, it should be possible to investigate the influence of different amino acids on biodistribution, as measured by bioluminescence. There are strong indications that the hydrophilicity of these substrates affects the pharmacodynamics and biodistribution in animals

ACKNOWLEDGMENT

We thank Timothy C. Doyle and Jonathan B. Rothbard (Stanford University) and Robert T. Taylor for critical review of the manuscript. We thank Sarah C. Chinn, Erica L. Gjersing, Julie L. Herberg, and Robert S. Maxwell (Lawrence Livermore National Laboratory) for assistance in obtaining NMR spectra.

SUPPORTING INFORMATION AVAILABLE

HPLC chromatograph of glycine-aminoluciferin **3** (Figure 1), absorbance spectra of the three substrates measured at 24 °C (Figure 2), fluorescence spectra of the three substrates measured at 24 °C (Figure 3), and bioluminescence emission spectra of the three substrates measured at 24 °C (Figure 4). This material is available free of charge via the Internet at http://pubs.acs.org.

REFERENCES

1. Contag, C. H., et al. (1995) Photonic detection of bacterial pathogens in living hosts, *Mol. Microbiol. 18* (4), 593−603.
2. Deluca, M. (1976) Firefly luciferase, *Adv. Enzymol. Relat. Areas Mol. Biol. 44*, 37−68.
3. Seliger, H. H., and McElroy, W. D. (1960) Spectral emission and quantum yield of firefly bioluminescence, *Arch. Biochem. Biophys. 88*, 136−41.
4. Koo, J. A., Schmidt, S. P., and Schuster, G. B. (1978) Bioluminescence of the firefly: Key steps in the formation of the electronically excited state for model systems, *Proc. Natl. Acad. Sci. U.S.A. 75* (1), 30−3.
5. Baggett, B., et al. (2004) Thermostability of firefly luciferases affects efficiency of detection by in vivo bioluminescence, *Mol. Imaging 3* (4), 324−32.
6. So, M. K., et al. (2006) Self-illuminating quantum dot conjugates for in vivo imaging, *Nat. Biotechnol*. (in press).
7. Liu, J. J., et al. (2005) Bioluminescent Imaging of TRAIL-Induced Apoptosis through Detection of Caspase Activation Following Cleavage of DEVD-Aminoluciferin, *Cancer Biol. Ther. 4* (8), 885−92.
8. O'Brien, M. A., et al. (2005) Homogeneous, bioluminescent protease assays: Caspase-3 as a model, *J. Biomol. Screening 10* (2), 137−48.
9. Shah, K., et al. (2005) In vivo imaging of S-TRAIL-mediated tumor regression and apoptosis, *Mol. Ther. 11* (6), 926−31.
10. Ignowski, J. M., and Schaffer, D. V. (2004) Kinetic analysis and modeling of firefly luciferase as a quantitative reporter gene in live mammalian cells, *Biotechnol. Bioeng. 86* (7), 827−34.
11. Lee, K. H., et al. (2003) Cell uptake and tissue distribution of radioiodine labelled D-luciferin: Implications for luciferase based gene imaging, *Nucl. Med. Commun. 24* (9), 1003−9.
12. Lee, S. Y., et al. (2004) Synthesis of 7′-[^{123}I]iodo-D-luciferin for in vivo studies of firefly luciferase gene expression, *Bioorg. Med. Chem. Lett. 14* (5), 1161−3.
13. Contag, C. H., et al. (1997) Visualizing gene expression in living mammals using a bioluminescent reporter, *Photochem. Photobiol. 66* (4), 523−31.
14. Cao, Y. A., et al. (2005) Molecular imaging using labeled donor tissues reveals patterns of engraftment, rejection, and survival in transplantation, *Transplantation 80* (1), 134−9.
15. Gross, S., and Piwnica-Worms, D. (2005) Real-time imaging of ligand-induced IKK activation in intact cells and in living mice, *Nat. Methods 2* (8), 607−14.
16. Chaudhari, A. J., et al. (2005) Hyperspectral and multispectral bioluminescence optical tomography for small animal imaging, *Phys. Med. Biol. 50* (23), 5421−41.
17. Katz, L. (1951) Antituberculous Compounds. II. 2-Benzalhydrazinobenzothiazoles, *J. Am. Chem. Soc. 73* (8), 4007−10.
18. White, E. H., et al. (1966) Amino Analogs of Firefly Luciferase and Biological Activity Thereof, *J. Am. Chem. Soc. 88*, 2015−9.
19. Monsees, T., Miska, W., and Geiger, R. (1994) Synthesis and characterization of a biolumogenic substrate for α-chymotrypsin, *Anal. Biochem. 221*, 329−34.
20. Troy, T., et al. (2004) Quantitative comparison of the sensitivity of detection of fluorescent and bioluminescent reporters in animal models, *Mol. Imaging 3* (1), 9−23.
21. Rice, B. W., Cable, M. D., and Nelson, M. B. (2001) In vivo imaging of light-emitting probes, *J. Biomed. Opt. 6* (4), 432−40.
22. Jenkins, D. E., et al. (2003) Bioluminescent imaging (BLI) to improve and refine traditional murine models of tumor growth and metastasis, *Clin. Exp. Metastasis 20* (8), 733−44.
23. Cao, Y. A., et al. (2004) Shifting foci of hematopoiesis during reconstitution from single stem cells, *Proc. Natl. Acad. Sci. U.S.A. 101* (1), 221−6.
24. White, E. H., et al. (1971) The chemi- and bioluminescence of firefly luciferin: An efficient chemical production of electronically excited states, *Bioorg. Chem. 1* (1−2), 92−122.

25. Zhao, H., et al. (2005) Emission spectra of bioluminescent reporters and interaction with mammalian tissue determine the sensitivity of detection in vivo, *J. Biomed. Opt. 10* (4), 41210.
26. White, E. H., et al. (1980) Chemi-Luminescence and Bioluminescence of Firefly Luciferin, *J. Am. Chem. Soc. 102* (9), 3199−208.
27. Gandelman, O., et al. (1994) Cytoplasmic factors that affect the intensity and stability of bioluminescence from firefly luciferase in living mammalian cells, *J. Biolumin. Chemilumin. 9* (6), 363−71.
28. Denburg, J. L., Lee, R. T., and McElroy, W. D. (1969) Substrate-binding properties of firefly luciferase. I. Luciferin-binding site, *Arch. Biochem. Biophys. 134* (2), 381−94.
29. Bennett, L. L., Ward, V. L., Jr., and Brockman, R. W. (1965) Inhibition of protein synthesis in vitro by cycloheximide and related glutarimide antibiotics, *Biochim. Biophys. Acta 103* (3), 478−85.
30. Gentry, R., Ye, L., and Nemerson, Y. (1995) A microscopic model of enzyme kinetics, *Biophys. J. 69* (2), 356−61.

BI060475O